EET Analog Treatment Improves Insulin Signaling in a Genetic Mouse Model of Insulin Resistance

Kakali Ghoshal,[1] Xiyue Li,[1] Dungeng Peng,[1] John R. Falck,[2] Raghunath Reddy Anugu,[2] Manuel Chiusa,[1] John M. Stafford,[3,4,5] David H. Wasserman,[3] Roy Zent,[1,5] James M. Luther,[6] and Ambra Pozzi[1,3,5]

We previously showed that global deletion of the cytochrome P450 epoxygenase *Cyp2c44*, a major epoxyeicosatrienoic acid (EET)–producing enzyme in mice, leads to impaired hepatic insulin signaling resulting in insulin resistance. This finding led us to investigate whether administration of a water-soluble EET analog restores insulin signaling in vivo in *Cyp2c44*$^{-/-}$ mice and investigated the underlying mechanisms by which this effect is exerted. *Cyp2c44*$^{-/-}$ mice treated with the analog disodium 13-(3-pentylureido)tridec-8(Z)-enoyl)-LL-aspartate2 (EET-A) for 4 weeks improved fasting glucose and glucose tolerance compared with *Cyp2c44*$^{-/-}$ mice treated with vehicle alone. This beneficial effect was accompanied by enhanced hepatic insulin signaling, decreased expression of gluconeogenic genes, and increased expression of glycogenic genes. Mechanistically, we show that insulin-stimulated phosphorylation of insulin receptor-β (IRβ) is impaired in primary *Cyp2c44*$^{-/-}$ hepatocytes and that this can be restored by cotreatment with EET-A and insulin. Plasma membrane fractionations of livers indicated that EET-A enhances the retention of IRβ in membrane-rich fractions, thus potentiating its activation. Altogether, EET analogs ameliorate insulin signaling in a genetic model of hepatic insulin resistance by stabilizing membrane-associated IRβ and potentiating insulin signaling.

Arachidonic acid (AA) is metabolized by cytochrome P450 (*CYP*) epoxygenase, and its oxidation by major epoxygenase isoforms (*CYP2C/2J*) results in the formation of four different epoxyeicosatrienoic acids (5,6-, 8,9-, 11,12-, and 14,15-EET) (1). EETs are hydrolyzed to less biologically active dihydroxyeicosatrienoic acids (DHETs) by epoxide hydrolases (e.g., soluble epoxide hydrolase [sEH] or *Ephx2*).

EETs regulate the activation and function of intracellular kinases, receptor tyrosine kinases, and anion channels, thus controlling vital cellular functions. In addition, EETs contribute to insulin sensitivity, thus providing a promising target in diabetes and metabolic complications. In humans, plasma EETs positively correlate with insulin sensitivity (2) and the *CYP2J2*7* loss-of-function variant is associated with earlier onset of type 2 diabetes (3), while a variant of EPHX2 (Arg287Gln) with decreased hydrolase activity is associated with increased insulin sensitivity (4). Animal studies indicate that *CYP2J3* gene therapy alleviates insulin resistance in *db/db* mice and in fructose-induced insulin-resistant rats (5). *CYP2J2* gene therapy in mice attenuates high-fat diet (HFD)–induced metabolic dysfunction by improving insulin sensitivity and reducing adipose tissue inflammation (6). In addition, the sEH inhibitor 1-(1-methylsulfonyl-piperidin-4-yl)-3-(4-trifluoromethoxy-phenyl)-urea (TUPS) attenuates HFD-induced insulin resistance (6).

Although these studies indicate that increasing CYP2C/J or decreasing sEH activity improves insulin signaling, the contribution of this pathway has been primarily investigated in pathological settings such as diabetes or obesity. The physiological role of EETs in regulating insulin signaling is less understood. In vitro studies show that treatment

of proximal renal tubular epithelial cells with 14,15-EET attenuates insulin-induced sodium–glucose cotransporter 2 expression, thus inhibiting glucose uptake (7). Chronic treatment of primary murine hepatocytes or HepG2 cells with high doses of EETs (30 μmol/L) improves insulin signaling and attenuates palmitate-induced insulin resistance (8). We previously showed that mice lacking Cyp2c44 show decreased hepatic insulin sensitivity and develop insulin resistance (2). As Cyp2c44 is a major generator of EETs in mice, we investigated whether treatment with stable EET analogs improves insulin signaling in this genetic model of hepatic insulin resistance and the mechanisms whereby the beneficial effects are exerted. We show that the EET analog disodium 13-(3-pentylureido)tridec-8(Z)-enoyl-L-aspartate2 (EET-A) (9) restores insulin signaling in $Cyp2c44^{-/-}$ mice and improves hepatic insulin signaling by potentiating insulin receptor-mediated signaling.

RESEARCH DESIGN AND METHODS

Animals
This study was conducted on 129/SvJ wild-type (WT) and $Cyp2c44^{-/-}$ male mice littermates, as described (10). Experiments were approved by the Vanderbilt Institutional Animal Care and Use Committee. Mice were provided a normal chow diet (Purina Laboratory Rodent 5001) and housed in an Association for Assessment and Accreditation of Laboratory Animal Care–accredited, temperature-controlled facility with a 12-h light/dark cycle.

In Vivo Treatment With EET-A
The water-soluble EET analog EET-A was based on the 14,15-EET scaffold and synthetized as previously described (9). This analog has been used in mice to test its effects on promoting angiogenesis (11) and ameliorating kidney injury (12).

Male mice (12–16 weeks old) were given access to water (vehicle) or EET-A (0.125 mg/mL in drinking water, which, for a mouse of ∼25 g that drinks 2 mL water/day, leads to a dose of 10 mg/kg body wt) for 4 weeks. For this study, we used $n = 29$ WT, vehicle; $n = 31$ $Cyp2c44^{-/-}$, vehicle; $n = 11$ WT, EET-A; and $n = 16$ $Cyp2c44^{-/-}$ EET-A mice.

Intraperitoneal Glucose Tolerance Test
An intraperitoneal glucose tolerance test (IPGTT) was performed before and after the treatment with EET-A following the National Mouse Metabolic Phenotyping Centers glucose tolerance test protocols (2). Mice fasted 5 h received an i.p. injection of 20% w/v glucose (final 2 g/kg body wt), and tail-vein blood glucose was measured at baseline, 15, 30, 45, 60, and 90 min. The area under the curve for glucose was calculated using the trapezoidal method.

Plasma samples were collected from 5-h fasted mice for glucose and insulin assay. Glucose was analyzed by enzymatic assay (CrystalChem, Elk Grove Village, IL).

Plasma insulin was determined by radioimmunoassay by the Vanderbilt Mouse Metabolic Phenotyping Center Analytical Core Laboratory. The updated HOMA of insulin resistance (HOMA2-IR) was calculated using fasting glucose and insulin (HOMA2 calculator v2.2, Oxford, U.K.) (13).

Evaluation of In Vivo Insulin Signaling in Liver and Muscle
Mice fasted 5 h were anesthetized and injected with insulin (Novolin R, 5 units) or vehicle (PBS) into the inferior vena cava, as described (14). After 15 min, the mice were sacrificed, and livers and gastrocnemius muscles were processed for RNA and/or Western blot analysis.

Insulin Signaling in Primary Hepatocytes
Mouse primary hepatocytes were isolated and cultured as described (15). Cells (1×10^6 cells/well in 6-well plates) were plated in M199 supplemented with 1% GlutaMAX, penicillin/streptomycin, 10% FBS, 10 nmol/L insulin, 100 nmol/L T3, and 500 nmol/L dexamethasone. After 4 h, cells were incubated in serum-free medium. After 12 h, cells were incubated with vehicle (water), EET-A (1 μmol/L), insulin (100 nmol/L), or a combination of insulin and EET-A for 30 min, and then processed for analysis of cell signaling. In some experiments, hepatocytes were pretreated with dansylcadaverine (50 μmol/L; Sigma-Aldrich, cat no. D4008-100MG) for 15 min, followed by insulin treatment (100 nmol/L) for 30 min and then processed for Western blot using selective primary antibodies (Supplementary Table 1).

Evaluation of Hepatic Glycogenic and Gluconeogenic Gene Expression
Liver RNA was extracted using TRIzol Reagent (Invitrogen). RNA (1 μg) was reverse transcribed to cDNA using iScript Reverse Transcription Supermix (Bio-Rad). Real-time (RT)-PCR was performed to evaluate the expression for glycogenic (glycogen synthase 2) and gluconeogenic (glucose 6-phosphatase, phosphoenolpyruvate carboxykinase, and fructose 1,6-bisphosphatase) genes. The primers and PCR conditions are described in Supplementary Table 2. Results are presented as fold-change normalized to GAPDH and WT expression using the $2^{-\Delta\Delta ct}$ method. The number of mice used was WT, $n = 17$; $2c44^{-/-}$, $n = 18$; WT+EET-A, $n = 5$; and $2c44^{-/-}$ +EET-A, $n = 10$.

Evaluation of Insulin Receptor Activation and Plasma Membrane Localization in $Cyp2c44^{-/-}$
Cytosol and plasma membrane-rich fractions from WT and $Cyp2c44^{-/-}$ livers were prepared as previously described (16). Liver tissues (200 mg) were incubated in Buffer A (50 mmol/L Tris·HCl [pH 8.0], 0.5 mmol/L dithiothreitol, 10 mmol/L NaF, 2 mmol/L Na_3VO_4, 0.1% [v/v] NP-40, and protease inhibitors), gently homogenized, passed through a 25-gauge needle, and centrifuged

for 1 min at 200g. The supernatant was collected and further centrifuged for 10 min at 800g and supernatant (A) and pellet (B) were collected. Supernatant A was further centrifuged for 20 min at 12,000g, and the new supernatant was saved as "cytosol-rich fraction." Pellet B was resuspended in buffer B (50 mmol/L Tris·HCl [pH 8.0], 0.5 mmol/L dithiothreitol, 10 mmol/L NaF, 2 mmol/L Na$_3$VO$_4$, 1% [v/v] NP-40, and protease inhibitors) and then centrifuged for 20 min at 12,000g, and the new supernatant was saved as "plasma membrane-rich fraction." Equal amounts of cytosol- and plasma membrane-rich fractions (20–60 μg) were used for Western blot analysis using the antibodies described in Supplementary Table 1.

Preparation of Tissue and Cell Lysates
Liver and hepatocyte lysates were prepared in radioimmunoprecipitation assay lysis buffer (Sigma-Aldrich, cat no. R0278-50ML) supplemented with EDTA-free Protease Inhibitor Cocktail (cOmplete) phosphatase inhibitors (Sigma-Aldrich), and 2 mnol/L Na$_3$VO$_4$. Lysates (40–50 μg) were separated by 10% v/v SDS-PAGE and transferred to 0.2 μm nitrocellulose membranes for Western blot analysis.

Western Blot Analysis and Quantification
Liver and hepatocyte lysates or liver fractions were incubated with the primary and secondary antibodies described in Supplementary Table 1. Bands were detected on Odyssey CLx (LI-COR Biosciences) or on GeneGnome XRQ, depending on the secondary antibody used. Bands were quantified by densitometric analysis using Image Studio Lite (LI-COR Biosciences) or GeneTools (Syngene), and values were expressed as phosphorylated protein-to-protein ratio.

Statistical Analysis
Data are presented as mean ± SD. Paired comparisons were made using the Wilcoxon signed rank test, and unpaired comparisons were made using Wilcoxon rank sum test. For GTT comparisons, generalized least squares regression and repeated measures with compound symmetry correlation were used to account for repeated measures in the same animal. All statistical analyses were conducted using R 4.0.2 software. A two-sided P value of <0.05 was considered significant.

Data and Resource Availability
The data sets generated during and/or analyzed during the current study are available from the corresponding author upon reasonable request. The $Cyp2c44^{-/-}$ mice analyzed during the current study are available from the corresponding author upon reasonable request.

RESULTS

EET-A Ameliorates Glucose Intolerance in $Cyp2c44^{-/-}$ Mice
To determine whether EET-A treatment improves glucose tolerance, we performed IPGTT on WT and $Cyp2c44^{-/-}$ mice before and after 4 weeks of treatment with vehicle or the EET analog EET-A. As previously reported (2), glucose tolerance was significantly impaired and fasting glucose was significantly higher in vehicle-treated $Cyp2c44^{-/-}$ mice compared with WT mice (Fig. 1A–C). EET-A treatment significantly improved glucose tolerance in $Cyp2c44^{-/-}$ mice but did not improve it in WT animals (Fig. 1A and B). Fasting glucose decreased in $Cyp2c44^{-/-}$ mice during EET-A treatment such that it was not significantly different from EET-A–treated WT mice (Fig. 1C). Although fasting insulin was similar in untreated WT and $Cyp2c44^{-/-}$ mice (0.61 ± 0.11 vs. 0.72 ± 0.15 ng/mL; $P = 0.23$) (Fig. 1D), insulin decreased in $Cyp2c44^{-/-}$ mice during EET-A treatment (0.57 ± 0.13 ng/mL, $P = 0.013$). Insulin resistance, as estimated by HOMA2-IR, was increased in untreated $Cyp2c44^{-/-}$ mice and decreased during EET-A treatment such that it did not differ significantly from EET-A–treated WT mice (Fig. 1E). EET-A treatment did not affect body weight (WT, vehicle = 25.74 ± 0.35 g; $Cyp2c44^{-/-}$, vehicle = 27.33 ± 0.54 g; WT, EET-A = 27.07 ± 0.55; $Cyp2c44^{-/-}$, EETA = 27.21 ± 0.94 g).

EET-A Treatment Ameliorates In Vivo Hepatic Insulin Signaling in $Cyp2c44^{-/-}$ Mice
To determine whether impaired hepatic insulin signaling contributes to the difference in glucose tolerance between WT and $Cyp2c44^{-/-}$ mice, we injected insulin or vehicle into the inferior vena cava of 5-h fasted WT and $Cyp2c44^{-/-}$ mice and then analyzed hepatic insulin signaling in liver excised 15 min after treatment. Insulin receptor-β (IRβ) was not activated in livers from vehicle-treated mice (Supplementary Fig. 1), as determined by IRβ Tyr1150 phosphorylation. Upon insulin stimulation, phosphorylation of this receptor was significantly higher in livers of WT than in $Cyp2c44^{-/-}$ mice, suggesting an impairment in hepatic insulin signaling in the latter group (Fig. 1F and G, Supplementary Fig. 1). Consistent with this finding, signaling downstream of the insulin receptor was enhanced by insulin in the livers of WT mice as reflected by significant increased phosphorylation of Akt (Ser473), FOXO1 (ser256), and glycogen synthase kinase-3β (GSK3β; Ser9) compared with insulin-treated $Cyp2c44^{-/-}$ mice (Fig. 1F and G, Supplementary Fig. 1). EET-A treatment significantly increased insulin-induced hepatic activation of insulin receptor and downstream signaling in $Cyp2c44^{-/-}$ mice (Fig. 1F and G), but it did not result in further enhancement of hepatic insulin signaling in WT mice. Thus, EET-A treatment enhances in vivo hepatic insulin signaling in conditions of $Cyp2c44^{-/-}$-induced insulin resistance.
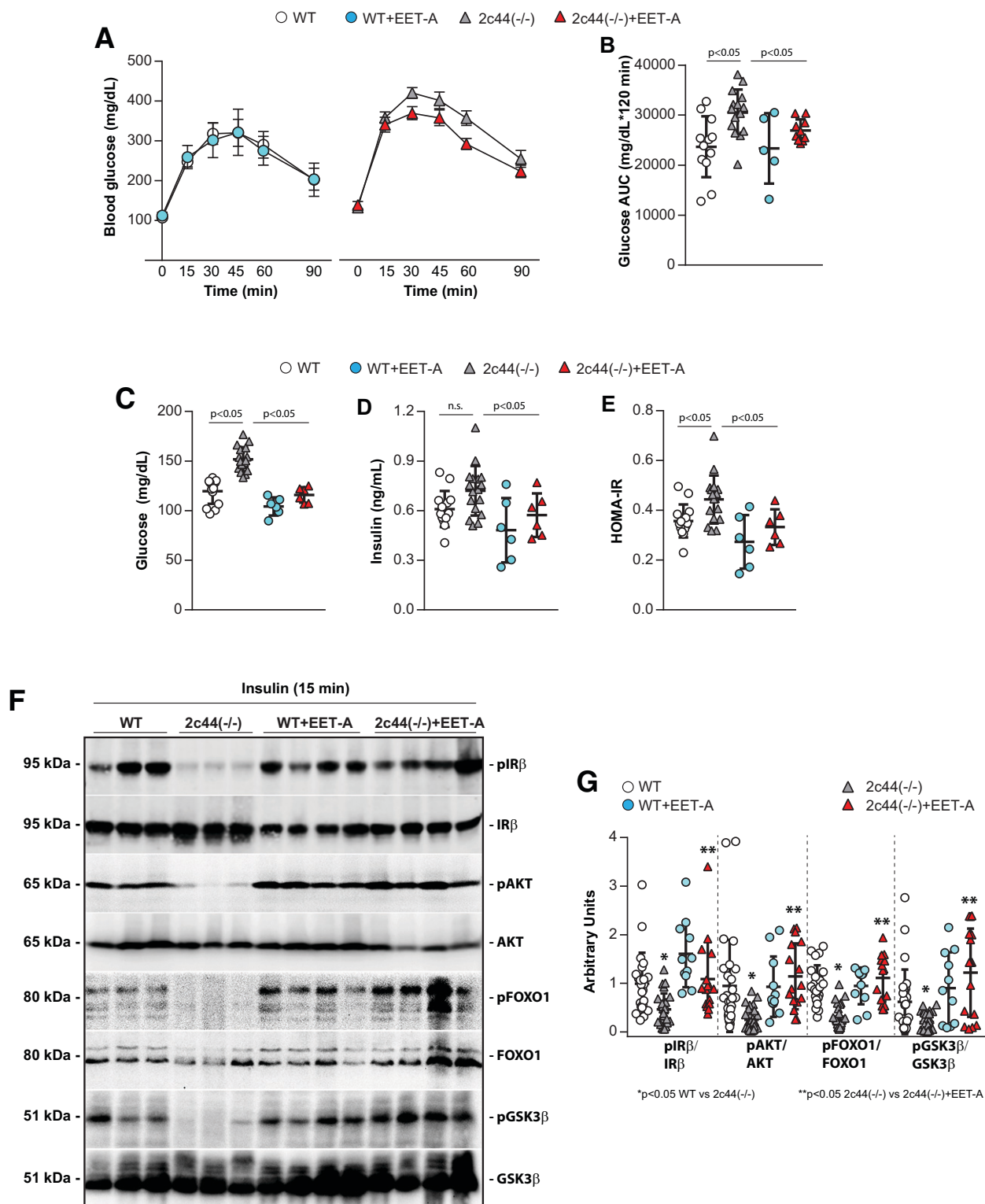
Figure 1—EET-A treatment restores hepatic insulin sensitivity in $Cyp2c44^{-/-}$ mice. IPGTT was performed in 5-h fasted WT and $Cyp2c44^{-/-}$ mice untreated (WT, $n = 12$; $2c44^{-/-}$, $n = 15$) or treated with EET-A in drinking water for 4 weeks (WT, $n = 5$; $2c44^{-/-}$, $n = 10$). IPGTT (A) and glucose area under the curve (AUC) (B) indicate that glucose tolerance was significantly impaired in untreated $Cyp2c44^{-/-}$ mice compared with untreated WT mice and that treatment with EET-A significantly improves glucose tolerance in the $Cyp2c44^{-/-}$ mice only. Fasting glucose (C), insulin (D), and insulin resistance estimated by HOMA2-IR (E) decreased significantly in $Cyp2c44^{-/-}$ mice and were similar to EET-A–treated WT mice. F: Mice fasted for 5 h received an injection of insulin via the inferior vena cava. Their livers were analyzed 15 min later by Western blot for insulin-mediated signaling ($n = 3$ mice are shown). Note the lack of insulin-receptor activation and insulin-mediated signaling in $Cyp2c44^{-/-}$ livers, which can be restored by EET-A treatment. G: Densitometry analysis of phosphorylated (p) and total protein bands was performed as described in the *Research Design and Methods*, and values are expressed as p-protein–to–total protein ratio. Values are the mean ± SD, and symbols represent individual mice.

Muscle Insulin Signaling Is Not Impaired in Cyp2c44⁻/⁻ Mice

We next determined whether Cyp2c44 plays a role in maintaining insulin signaling in tissues other than liver, such as muscle. Gastrocnemius muscles were collected from 5 h-fasted WT and $Cyp2c44^{-/-}$ mice injected with insulin (5 units) or vehicle, as described above. No activation of IRβ was detected in the muscle of vehicle-treated mice (Supplementary Fig. 2A and B). However, upon insulin stimulation, Tyr1150 phosphorylation of the insulin receptor was detected in the muscle of both WT and $Cyp2c44^{-/-}$ mice (Supplementary Fig. 2A and B). Consistent with this finding, signaling downstream of the insulin receptor, such as phosphorylation of Akt (Ser473) and FOXO1 (ser256), was activated equally in the muscle of WT and $Cyp2c44^{-/-}$ mice (Supplementary Fig. 2C–F). Although insulin stimulated GSK3β activation (Ser9) in the muscle of both WT and $Cyp2c44^{-/-}$ mice, differences did not reach significance in insulin- versus vehicle-treated mice (Supplementary Fig. 2G and H). EET-A treatment did not significantly increase insulin-induced activation of the insulin receptor in muscle and downstream signaling in WT or $Cyp2c44^{-/-}$ mice (Supplementary Fig. 2), similar to the results obtained with hepatic insulin signaling in WT mice.

EET-A Treatment Decreases Hepatic Gluconeogenic and Enhances Glycogenic Gene Expression in Cyp2c44⁻/⁻ Mice

Insulin signaling inhibits hepatic gluconeogenesis by negatively regulating the expression of fructose-1,6-bisphosphatase (F1,6Pase), glucose 6-phosphatase (G6Pase), and phosphoenolpyruvate carboxykinase (PEPCK) (Fig. 2A). This is exerted by insulin-mediated phosphorylation of the transcription factor FOXO1 on Ser253, thus preventing its nuclear translocation and activation of gluconeogenesis genes. In addition, insulin promotes glycogen synthesis by promoting AKT-mediated phosphorylation of GSK3β on Ser9, thus preventing GSK3β-mediated inhibition of glycogen synthase 2 (GS2) (Fig. 2A). RNA analysis of genes whose products regulate gluconeogenesis and glyconeogenesis in the livers of vehicle-treated WT and $Cyp2c44^{-/-}$ mice revealed significantly higher levels of G6Pase and PEPCK mRNA and significantly lower levels of GS2 mRNA in $Cyp2c44^{-/-}$ livers compared with WT livers (Fig. 2B–E). EET-A treatment significantly reduced the mRNA levels of G6Pase and PEPCK and significantly increased mRNA levels of GS2 in $Cyp2c44^{-/-}$ livers (Fig. 2B–E). We did not observe a difference in F1,6Pase mRNA expression between WT and $Cyp2c44^{-/-}$ mice treated with vehicle alone; however, EET-A treatment significantly reduced F1,6Pase expression in $Cyp2c44^{-/-}$ (Fig. 2C). Thus, EET-A treatment improves glucose tolerance in the $Cyp2c44^{-/-}$ mice, potentially by increasing glyconeogenesis and decreasing gluconeogenesis genes.

EET-A Restores Insulin Sensitivity in Isolated Primary Hepatocytes of Cyp2c44⁻/⁻ Mice

To further analyze the mechanisms whereby EET-A promotes insulin signaling, we isolated primary hepatocytes from WT and $Cyp2c44^{-/-}$ that were cultured in serum-free medium for 12 h and then treated with vehicle, EET-A (1 μmol/L), insulin (100 nmol/L), or a combination of EET-A and insulin. After 30 min, cell lysates were analyzed for levels of IRβ activation and downstream signaling. No phosphorylation of IRβ (Tyr1150), AKT (Ser473), FOXO1 (Ser256), or GSK3β (Ser9) was detected in hepatocytes treated with vehicle alone. Insulin treatment induced activation of IRβ and downstream signaling in WT but not in $Cyp2c44^{-/-}$ hepatocytes (Fig. 3A and B), consistent with the in vivo reduced hepatic insulin signaling observed in $Cyp2c44^{-/-}$ mice (Fig. 1). Treatment of cells with EET-A alone did not activate IRβ or downstream signaling in WT or $Cyp2c44^{-/-}$ hepatocytes (Fig. 3A–H). However, EET-A given together with insulin significantly enhanced IRβ and/or downstream signaling in $Cyp2c44^{-/-}$ hepatocytes compared with $Cyp2c44^{-/-}$ cells treated with EET-A or insulin alone (Fig. 3A–H). Although EET-A increased insulin-mediated activation of IRβ and/or downstream signaling in WT hepatocytes, differences were not significant when compared with WT hepatocytes treated with insulin alone (Fig. 3A–H). Thus, EET-A significantly potentiates insulin-mediated signaling only in mouse hepatocytes lacking the $Cyp2c44^{-/-}$ gene.

EET-A Enhances the Retention of Activated Insulin Receptor on Liver Plasma Membrane

Insulin-mediated IRβ phosphorylation leads to receptor internalization and lysosome-mediated degradation (17). Accelerated insulin-induced receptor internalization can lead to insulin resistance (17). Thus, we isolated plasma membrane-rich fractions of livers from WT and $Cyp2c44^{-/-}$ mice treated with vehicle for 15 min and confirmed their purity by analyzing the levels and distributions of the Na/K ATPase (a plasma membrane marker), α-tubulin (a cytosol maker), calnexin (an endoplasmic reticulum marker), and syntaxin 6 (a Golgi maker) (Supplementary Fig. 1I and J). Then, we analyzed the levels of total IRβ in plasma membrane-rich fractions of livers from mice treated with vehicle or insulin for 15 min. No differences in plasma membrane-associated IRβ levels were observed between vehicle-treated WT and $Cyp2c44^{-/-}$ livers (Fig. 4A and B). Upon insulin treatment, we detected a significant decrease in plasma membrane-associated IRβ in WT and $Cyp2c44^{-/-}$ livers; however, this effect was more pronounced in $Cyp2c44^{-/-}$ livers (Fig. 4A and B). To determine whether EET-A can affect the plasma membrane localization of IRβ, we analyzed the levels of plasma membrane-associated IRB in the livers of $Cyp2c44^{-/-}$ mice untreated or treated with EET-A for 4 weeks upon 15-min insulin stimulation. A significant increase in plasma membrane-associated IRβ was observed in the livers of EET-A–treated $Cyp2c44^{-/-}$
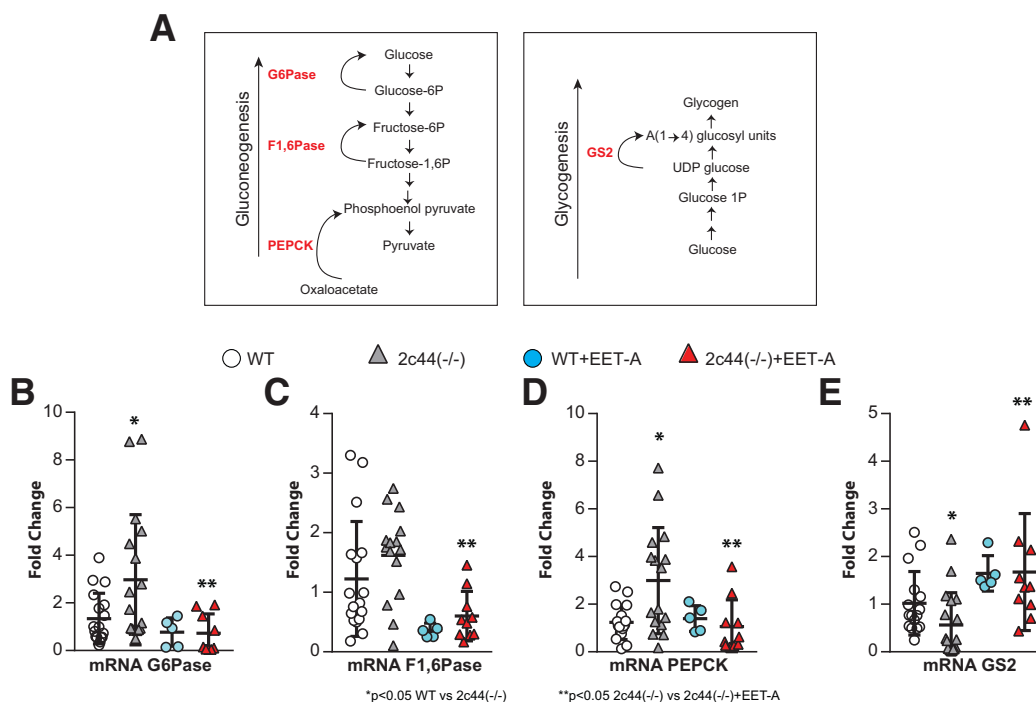
Figure 2—EET-A treatment decreases gluconeogenic and enhances glycogenic gene expression in liver of $Cyp2c44^{-/-}$ mice. *A*: Schematic representation of the gluconeogenesis and glycogenesis pathways showing insulin-regulated enzymes in red. UDP, uridine diphosphate glucose. RT-PCR analysis of GP6Pase (*B*) F1,6Pase (*C*), PEPCK (*D*), and GS2 (*E*) mRNA levels in livers from WT and $Cyp2c44^{-/-}$ untreated (WT, $n = 17$; $2c44^{-/-}$, $n = 18$) or treated for 4 weeks with EET-A (WT, $n = 5$; $2c44^{-/-}$, $n = 10$). Values are the mean ± SD and are expressed as fold-change for the gene expression with GAPDH as the housekeeping gene. Symbols represent individual mice.

compared with untreated mice upon insulin stimulation (Fig. 4*C* and *D*), and this was also accompanied by increased levels of plasma membrane–associated phosphorylated IRβ receptor (Fig. 4*E* and *F*). To confirm the in vivo results, we investigated the phosphorylation of IRβ in hepatocytes from $Cyp2c44^{-/-}$ mice treated with vehicle, EET-A, insulin, EETA + insulin, or insulin + dansylcadaverine, an inhibitor of activated IRβ internalization (18). Only cotreatment of hepatocytes with dansylcadaverine or EET-A significantly enhanced insulin-mediated IRβ and downstream AKT phosphorylation (Fig. 4*G–I*), suggesting that one mechanism by which EET-A promotes insulin signaling is by decreasing insulin-mediated receptor internalization, which thereby potentiates insulin signaling.

DISCUSSION

Insulin resistance is a primary risk factor for development of type 2 diabetes, cardiovascular disease, and dyslipidemias, and impaired EET generation or increased degradation worsens insulin sensitivity. Cyp2c44 contributes to EET generation, and its genetic deletion results in systemic and hepatic insulin resistance. Because reduced EET production and other compensatory effects of *Cyp2c44* deletion can contribute to development of insulin resistance, we determined the role of EET analog treatment in the setting of insulin resistance in $Cyp2c44^{-/-}$ mice. We

show that the EET analog EET-A improves hepatic insulin action in these mice by enhancing insulin receptor–mediated signaling, which suggests that that EET analogs might be a therapeutic option for the treatment of insulin resistance due to reduced epoxygenase activity.

Increased bioavailability of EETs is dependent on increased *CYP2C/J* or decreased sEH expression and activity. In mice, inhibition or deletion of sEH promotes glucose-stimulated insulin secretion from β-cells and prevents islet apoptosis, hyperglycemia, and insulin resistance (19). Pharmacological inhibitors of sEH reduce hyperglycemia in insulin-resistant rats (20). In addition, increased sEH and reduced *CYP2C11* and *CYP2J* expression and activity are observed in an obesity-induced diabetic rat model or 3-week HFD-fed mice (21,22). Consistent with a role of the Cyp2c/EET axis in regulating insulin sensitivity, mice lacking hemoxygenase 2 are insulin resistant and produce less renal EETs than WT mice (23). Treatment with the EET analog (*S*)-2-(11-(nonyloxy)undec-8(*Z*)-enamido) succinic acid (NUDSA) ameliorates insulin resistance in part due to increased *Cyp2c44* expression and EET production (23). Although these studies highlight the importance of CYP2C/J and sEH in the management of hyperglycemia or diabetes, most of them were conducted in a high fat–induced and/or diabetic environment and did not investigate the molecular mechanisms whereby these enzymes and their products exerts their effects on insulin
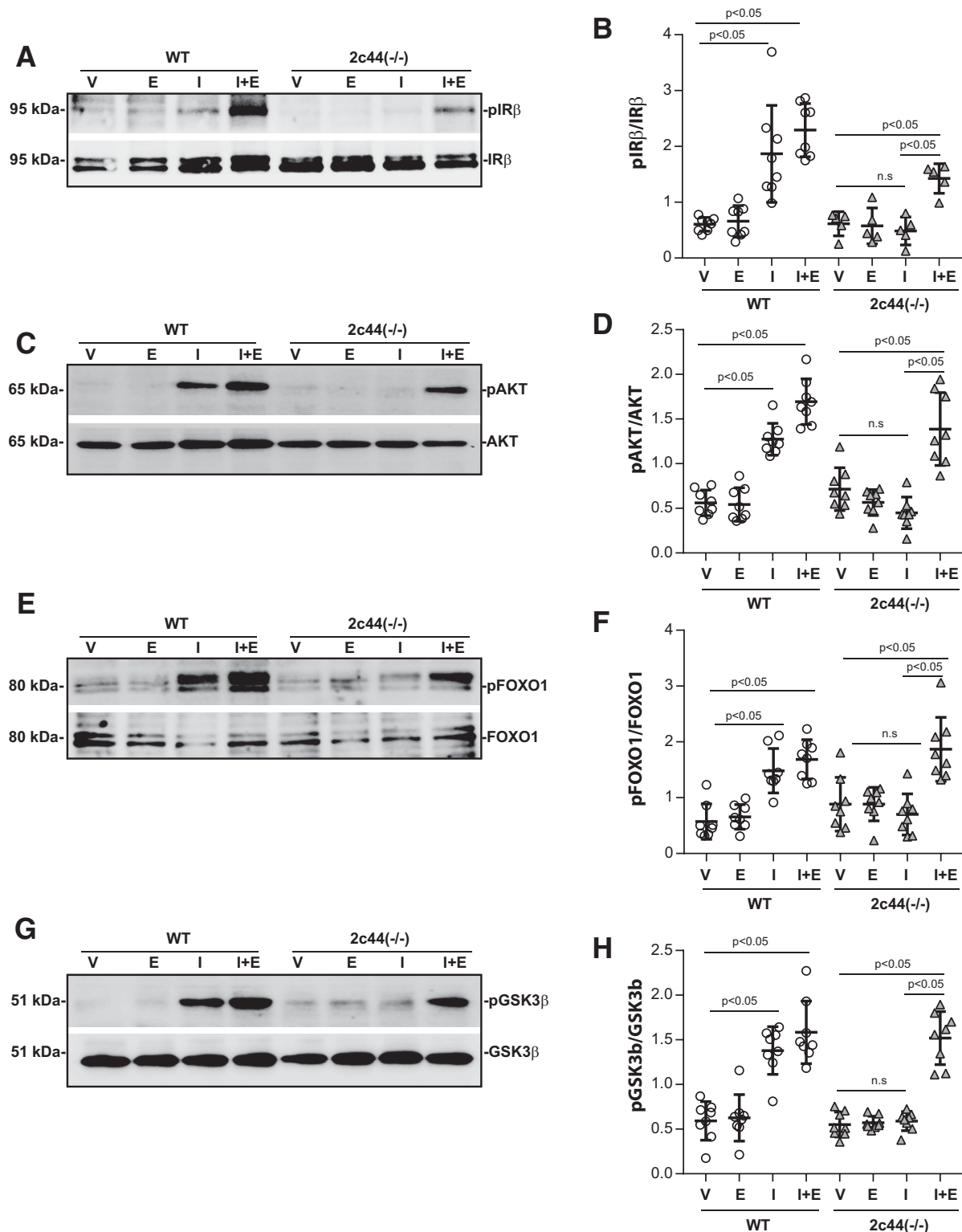
Figure 3—EET-A treatment restores insulin sensitivity in primary *Cyp2c44*$^{-/-}$ hepatocytes. WT and *Cyp2c44*$^{-/-}$ primary hepatocytes serum starved for 12 h were treated with vehicle (V), EET-A (E, 1 μmol/L) insulin (I, 100 nmol/L), or insulin with EET-A (I+E). After 30 min, cell lysates were analyzed by Western blot for levels of activated (phosphorylated [p]) and total IRβ (*A*), AKT (*C*), FOXO1 (*E*), and GSK3β (*G*). *B*, *D*, *F*, and *H*: Bands were quantified by densitometry as described in the *Research Design and Methods*, and values are expressed as p-protein–to–total protein ratio. Values are the mean ± SD, and symbols represent individual livers. Note that insulin fails to activate IRβ and downstream signaling in *Cyp2c44*$^{-/-}$ hepatocytes and that this effect is potentiated by cotreatment with EET-A.
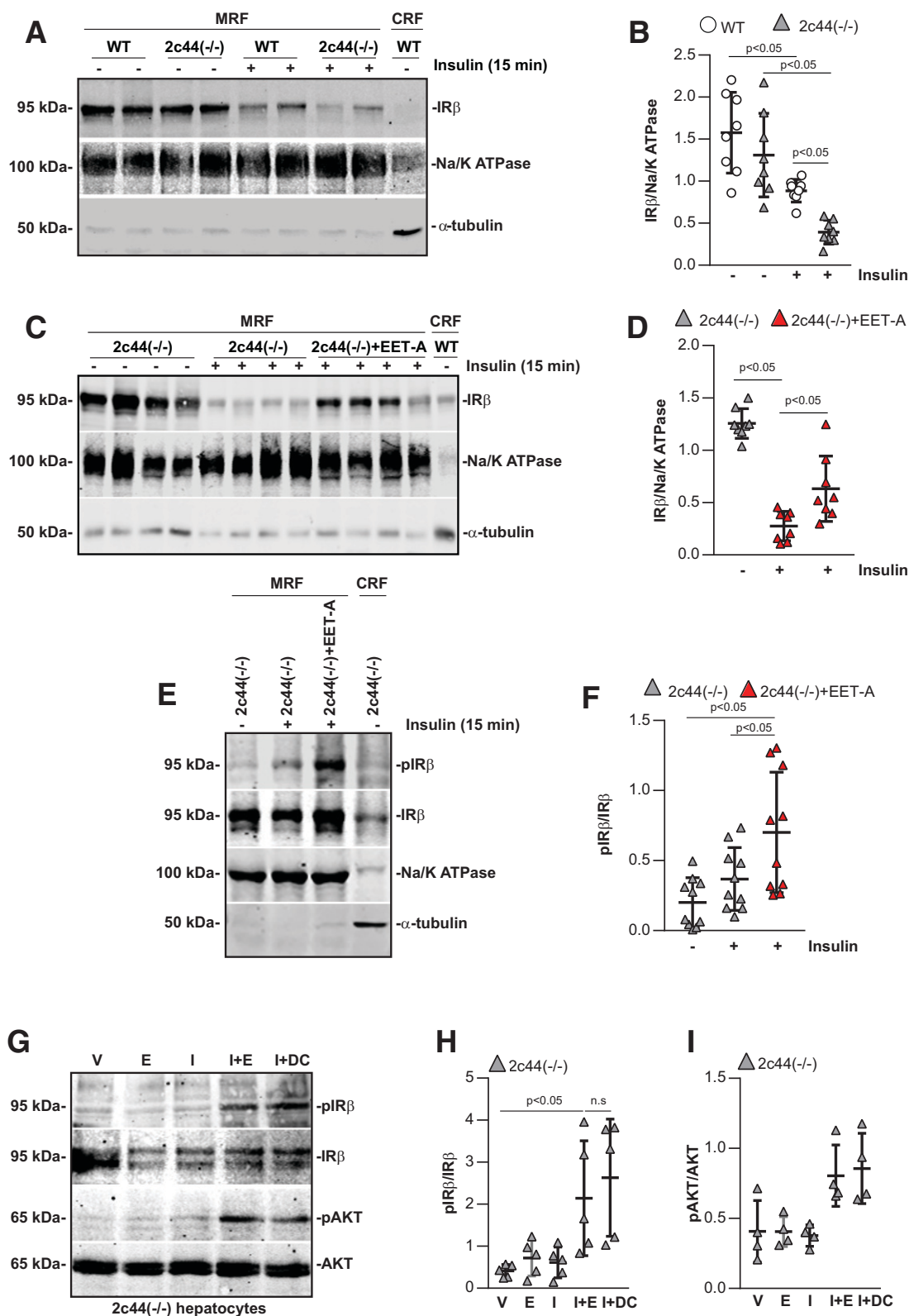
Figure 4—EET-A increases membrane-associated IRβ in livers of *Cyp2c44*$^{-/-}$ mice. *A*, *C*, and *E*: Membrane rich (MRF) or cytosol rich (CRF) fractions were isolated from livers of the mice indicated as untreated or treated with insulin, as described in Fig. 1. Fractions were then analyzed by Western blot for levels of total or phosphorylated (p)IRβ. Na/K ATPase and α-tubulin were used to verify the purity of the fractions. *B*, *D*, and *F*: Densitometry analysis of phosphorylated or total IRβ bands was performed as described in the *Research Design and Methods*, and values are expressed as the IRβ–to–Na/K ATPase or pIRβ-to-IRβ ratio. Values are the mean ± SD, and symbols represent individual livers. *G*: Primary *Cyp2c44*$^{-/-}$ hepatocytes were treated with vehicle (V), EET-A (E, 1 μmol/L) insulin (I, 100 nmol/L), insulin with EET-A (I+E), or insulin and dansylcadaverine (I+DC, 50 μmol/L). After 30 min, cell lysates were analyzed by Western blot for levels of activated and total IRβ or AKT. *H* and *I*: Bands were quantified by densitometry as described in the *Research Design and Methods*, and values expressed as the p-protein–to–total protein ratio. Values are the mean ± SD, and symbols represent individual livers.

signaling. Although sEH inhibitors are in development, these drugs may affect multiple metabolites. EET analogs are therefore an attractive alternative. Our current study demonstrates an effect on hepatic insulin sensitivity, which could make development of a liver-specific drug (e.g., oral delivery with high first-pass hepatic metabolism) attractive to avoid unnecessary systemic exposure.

EETs might promote insulin signaling by activating downstream signaling activated by the insulin receptor, such as AKT. Interestingly, treatment of primary WT mouse hepatocytes with 4 μmol/L of each EET regio-isomer promotes AKT signaling and potentiates low-dose insulin-stimulated AKT activation (22). EET-mediated AKT activation is exerted without affecting insulin receptor phosphorylation, suggesting that EETs work downstream of the insulin receptor (22). In contrast to this finding, we show that treatment of WT mouse hepatocytes with 1 μmol/L of the EET analog EET-A is not sufficient to promote AKT activation and does not potentiate insulin signaling. A possible explanation for this discrepancy is the dose of EET used (4 μmol/L vs. 1 μmol/L in our study), the duration of the treatment (60 min vs. 30 min in our study), or the fact that EET-enhanced insulin-mediated signaling was observed when low-dose insulin was used (1.5 nmol/L vs. 100 nmol/L in our study).

EETs might regulate intracellular signaling by directly crossing the plasma membrane and incorporating into phospholipids (24). To this end, P450 eicosanoids can bind to and activate peroxisome proliferator–activated receptor-α (PPAR-α), thus regulating PPAR-α target gene expression (25). In addition, EETs could exert their biological function by binding the low affinity EET receptor GPR40 (26) and activating intracellular kinases or potentiating receptor tyrosine kinase-mediated activation of intracellular kinases. A key finding in this study is that in the liver, EETs enhance the plasma membrane localization of the activated insulin receptor, thus increasing receptor activation and downstream signaling. Upon insulin binding, the insulin receptor is internalized by a clathrin-mediated endocytosis (27), and fast insulin receptor internalization is linked to insulin resistance (17). We show that the plasma membrane-associated levels of insulin receptor in the livers of WT and $Cyp2c44^{-/-}$ mice treated with insulin are lower than plasma membrane-associated receptor levels in mice treated with vehicle alone, with the lowest levels observed in the insulin-treated $Cyp2c44^{-/-}$ livers. The finding that EET-A increases the levels of plasma membrane associated hepatic insulin receptor in insulin-treated $Cyp2c44^{-/-}$ mice to those observed following treatment with dansylcadaverine, an inhibitor of clathrin-mediated IRβ internalization (18), suggests that EETs increase the stabilization of activated hepatic insulin receptor to the plasma membrane thus potentiating its action.

Our study does not support an effect of Cyp2c44 deletion on muscle insulin signaling. A possible explanation is

that $Cyp2c44$ expression measured by Affymetrix and RNA sequencing is lower in muscle than in the liver (expression score 57.22 vs 99.39 respectively, https://bgee.org/?page=gene&gene_id=ENSMUSG00000025197). Thus, muscle Cyp2c44-derived EETs might not be involved in regulating localization and function of the IRβ.

In conclusion, our findings show that administration of an EET analog is beneficial in insulin resistance by restoring hepatic insulin signaling in a mouse and may have potential for translation to insulin resistance in human subjects.

Author Contributions. K.G. conducted experiments, acquired data, analyzed data, and wrote the manuscript. X.L., D.P., and M.C. conducted experiments. J.R.F. and R.R.A. provided reagents. J.M.S., D.H.W., R.Z., and J.M.L. contributed to discussion and reviewed and edited the manuscript. A.P. designed research studies and wrote the manuscript. A.P. is the guarantor of this work and, as such, had full access to all the data in the study and takes responsibility for the integrity of the data and the accuracy of the data analysis.

References

1. Capdevila JH, Dishman E, Karara A, Falck JR. Cytochrome P450 arachidonic acid epoxygenase: stereochemical characterization of epoxyeicosatrienoic acids. Methods Enzymol 1991;206:441–453

2. Gangadhariah MH, Dieckmann BW, Lantier L, et al. Cytochrome P450 epoxygenase-derived epoxyeicosatrienoic acids contribute to insulin sensitivity in mice and in humans. Diabetologia 2017;60:1066–1075

3. Wang CP, Hung WC, Yu TH, et al. Genetic variation in the G-50T polymorphism of the cytochrome P450 epoxygenase *CYP2J2* gene and the risk of younger onset type 2 diabetes among Chinese population: potential interaction with body mass index and family history. Exp Clin Endocrinol Diabetes 2010;118:346–352

4. Ramirez CE, Shuey MM, Milne GL, et al. Arg287Gln variant of *EPHX2* and epoxyeicosatrienoic acids are associated with insulin sensitivity in humans. Prostaglandins Other Lipid Mediat 2014;113-115:38–44

5. Xu X, Zhao CX, Wang L, et al. Increased CYP2J3 expression reduces insulin resistance in fructose-treated rats and db/db mice. Diabetes 2010; 59:997–1005

6. Dai M, Wu L, Wang P, Wen Z, Xu X, Wang DW. CYP2J2 and its metabolites EETs attenuate insulin resistance via regulating macrophage polarization in adipose tissue. Sci Rep 2017;7:46743

7. Fu M, Yu J, Chen Z, et al. Epoxyeicosatrienoic acids improve glucose homeostasis by preventing NF-κB-mediated transcription of SGLT2 in renal tubular epithelial cells. Mol Cell Endocrinol 2021;523:111149

8. Skepner JE, Shelly LD, Ji C, Reidich B, Luo Y. Chronic treatment with epoxyeicosatrienoic acids modulates insulin signaling and prevents insulin resistance in hepatocytes. Prostaglandins Other Lipid Mediat 2011;94:3–8

9. Falck JR, Kodela R, Manne R, et al. 14,15-Epoxyeicosa-5,8,11-trienoic acid (14,15-EET) surrogates containing epoxide bioisosteres: influence upon vascular relaxation and soluble epoxide hydrolase inhibition. J Med Chem 2009;52:5069–5075

10. Pozzi A, Popescu V, Yang S, et al. The anti-tumorigenic properties of peroxisomal proliferator-activated receptor alpha are arachidonic acid epoxygenase-mediated. J Biol Chem 2010;285:12840–12850

11. Skrypnyk N, Chen X, Hu W, et al. PPARα activation can help prevent and treat non-small cell lung cancer. Cancer Res 2014;74:621–631

12. Khan MA, Liu J, Kumar G, Skapek SX, Falck JR, Imig JD. Novel orally active epoxyeicosatrienoic acid (EET) analogs attenuate cisplatin nephro-toxicity. FASEB J 2013;27:2946–2956

13. Levy JC, Matthews DR, Hermans MP. Correct homeostasis model assessment (HOMA) evaluation uses the computer program. Diabetes Care 1998;21:2191–2192

14. Chaudhari A, Ejeskär K, Wettergren Y, Kahn CR, Rotter Sopasakis V. Hepatic deletion of p110α and p85α results in insulin resistance despite sustained IRS1-associated phosphatidylinositol kinase activity. F1000 Res 2017;6:1600

15. Foretz M, Hébrard S, Leclerc J, et al. Metformin inhibits hepatic gluconeogenesis in mice independently of the LKB1/AMPK pathway via a decrease in hepatic energy state. J Clin Invest 2010;120:2355–2369

16. Yamamoto N, Yamashita Y, Yoshioka Y, Nishiumi S, Ashida H. Rapid preparation of a plasma membrane fraction: Western blot detection of translocated glucose transporter 4 from plasma membrane of muscle and adipose cells and tissues. Curr Protoc Protein Sci 2016;85:29.18.1–29.18.12

17. Chen Y, Huang L, Qi X, Chen C. Insulin receptor trafficking: consequences for insulin sensitivity and diabetes. Int J Mol Sci 2019;20:5007

18. Ugi S, Shi K, Nishio Y, et al. Membrane localization of protein-tyrosine phosphatase 1B is essential for its activation of sterol regulatory element-binding protein-1 gene expression and consequent hypertriglyceridaemia. J Biochem 2009;146:541–547

19. Luria A, Bettaieb A, Xi Y, et al. Soluble epoxide hydrolase deficiency alters pancreatic islet size and improves glucose homeostasis in a model of insulin resistance. Proc Natl Acad Sci U S A 2011;108:9038–9043

20. Guglielmino K, Jackson K, Harris TR, et al. Pharmacological inhibition of soluble epoxide hydrolase provides cardioprotection in hyperglycemic rats. Am J Physiol Heart Circ Physiol 2012;303:H853–H862

21. Zhao X, Dey A, Romanko OP, et al. Decreased epoxygenase and increased epoxide hydrolase expression in the mesenteric artery of obese Zucker rats. Am J Physiol Regul Integr Comp Physiol 2005;288:R188–R196

22. Schäfer A, Neschen S, Kahle M, et al. The epoxyeicosatrienoic acid pathway enhances hepatic insulin signaling and is repressed in insulin-resistant mouse liver. Mol Cell Proteomics 2015;14:2764–2774

23. Sodhi K, Inoue K, Gotlinger KH, et al. Epoxyeicosatrienoic acid agonist rescues the metabolic syndrome phenotype of HO-2-null mice. J Pharmacol Exp Ther 2009;331:906–916

24. Spector AA. Arachidonic acid cytochrome P450 epoxygenase pathway. J Lipid Res 2009;50(Suppl.):S52–S56

25. Ng VY, Huang Y, Reddy LM, Falck JR, Lin ET, Kroetz DL. Cytochrome P450 eicosanoids are activators of peroxisome proliferator-activated receptor alpha. Drug Metab Dispos 2007;35:1126–1134

26. Park SK, Herrnreiter A, Pfister SL, et al. GPR40 is a low-affinity epoxyeicosatrienoic acid receptor in vascular cells. J Biol Chem 2018;293:10675–10691

27. Goh LK, Sorkin A. Endocytosis of receptor tyrosine kinases. Cold Spring Harb Perspect Biol 2013;5:a017459